FULL PAPER

Dalton
www.rsc.org/dalton

Ruthenium(II) complexes containing asymmetric ligands: synthesis, characterization, crystal structure and DNA-binding

Hong Deng,[a] Jiwen Cai,[a] Hong Xu,[a] Hao Zhang[a] and Liang-Nian Ji*[a,b]

[a] *School of Chemistry and Chemical Engineering, State Key Laboratory of Optoelectronic Materials and Technologies, Zhongshan University, Guangzhou 510275, P. R. China*

[b] *State Key Laboratory of Bio-organic, Natural Products Chemistry of Shanghai Institute of Organic Chemistry, Shanghai 200032, P. R. China*

Received 29th August 2002, Accepted 2nd December 2002
First published as an Advance Article on the web 9th January 2003

Two new asymmetric ligands, 3-(pyrazin-2-yl)-*as*-triazino[5,6-*f*]acenaphthylene (dta) and 3-(pyrazin-2-yl)-*as*-triazino[5,6-*f*]phenanthrene (dpt) and three novel ruthenium(II) complexes $[Ru(bpy)_2(L)][ClO_4]_2$ (bpy = 2,2′-bipyridine, L = ddt (**1**), dta (**2**) and dpt (**3**), ddt = 3-(pyrazin-2-yl)-5,6-diphenyl-*as*-triazine) have been synthesized and characterized by mass spectroscopy, ^{1}H NMR and cyclic voltammetry. The crystal structures of dta and $[Ru(bpy)_2(ddt)][ClO_4]_2$ (**1**) were also determined. Interactions of the complexes with calf thymus DNA have also been investigated by spectrophotometric and viscosity measurements. The planar extension of the intercalative ligand increases the interaction of the complex with DNA, indicating that the size and shape of the intercalated ligand have a marked effect on the strength of interaction. The circular dichroism signals of the dialysates of the racemic complexes against calf thymus DNA suggest that complexes **2** and **3** interact enantioselectively with calf thymus DNA, but not complex **1**. Complexes **2** and **3** have been found to promote the cleavage of plasmid pBR 322 DNA from the supercoiled form I to the open circular form II upon irradiation.

Introduction

Ruthenium(II) polypyridyl complexes have aroused intense interest because of their extensive applications in the fields of photochemistry, photophysics and biochemistry. In particular, their important application for probes of DNA structure, DNA mediated electron transfer, DNA footprinting and sequence-specific cleaving agents is well known.[1] The strong absorbance caused by metal-to-ligand charge transfer (MLCT), the luminescent characteristics and their perturbations upon binding to DNA of the Ru(II) complexes provide practicable means to explore their DNA binding mechanisms. Over the past decade, quite a large amount of research has been carried out in relation to these subjects.[2]

However, most of the reported complexes contain symmetric aromatic ligands and they are structural analogues based on the prototype $[Ru(phen)_3]^{2+}$. There are only a limited number of ruthenium complexes containing asymmetric ligands and little attention has been paid to the investigation of their DNA-binding properties. In fact, some of these complexes also exhibit interesting properties upon binding to DNA. For example, $[Ru(bpy)_2(pztp)][ClO_4]_2$ (pztp = 3-(pyrazin-2-yl)-*as*-triazino-[5,6-*f*]1,10-phenanthroline) intercalates the base pairs of DNA and $[Ru(bpy)_2(dpp)][ClO_4]_2$ (dpp = 2,3-di-2-pyridylpyrazine) binds to DNA by electrostatic interactions.[3,4]

Because the octahedral mixed-ligand ruthenium(II) complexes can be modified in three dimensions to adapt to the DNA helix,[5,6] the shape of the ligand plays a key role in the interaction with DNA.[7] We have been interested in synthesizing new polypyridyl ruthenium(II) complexes and studying their interaction properties with DNA, aiming to elucidate their binding mechanism.[8] Herein, in order to obtain more insights into the DNA-binging properties of ruthenium(II) complexes with asymmetric ligands, and investigate the influence of the ligand on DNA-binding affinity, three novel ruthenium complexes $[Ru(bpy)_2(ddt)][C1O_4]_2$ **1** (bpy = 2,2′-bipyridine, ddt = 3-(pyrazin-2-yl)-5,6-diphenyl-*as*-triazine, Scheme 1), $[Ru(bpy)_2(dta)][C1O_4]_2$ **2** (dta = 3-(pyrazin-2-yl)-*as*-triazino[5,6-*f*]-acenaphthylene, Scheme 1) and $[Ru(bpy)_2(dpt)][C1O_4]_2$ **3** (dpt = 3-(pyrazin-2-yl)-*as*-triazino[5,6-*f*]phenanthrene, Scheme 1) were synthesized and characterized. Their interactions with DNA were explored by electronic absorption, viscosity and circular dichroism measurements. The abilities of these Ru(II) complexes to induce the cleavage of pBR 322 DNA were also investigated.

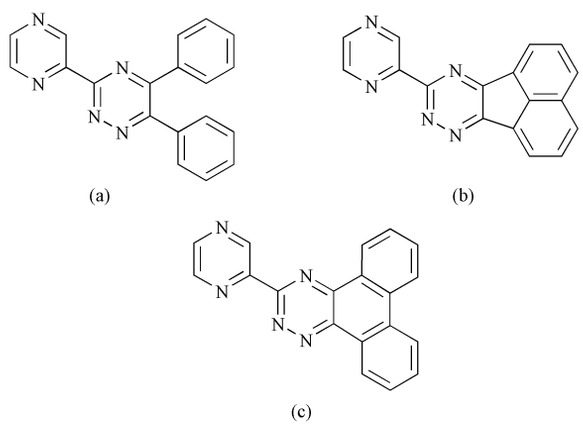

Scheme 1 Structure of the ligands ddt (a), dta (b), dpt (c).

Experimental

Synthesis

cis-$[Ru(bpy)_2Cl_2]\cdot 2H_2O$[9] and cyanodiazine hydrazidine[10] were prepared according to the literature procedures, and other chemicals were commercially available.

3-(Pyrazin-2-yl)-5,6-diphenyl-*as*-triazine (ddt)

ddt was synthesized using the method described by Case[10] and further confirmed by NMR spectroscopy. Yield: 0.534 g, 86%. ^{1}H NMR (CD_2Cl_2): δ 9.92 (s, 1H), 8.89 (d, 1H, J = 5.0), 8.79 (d, 1H, J = 6.5), 7.70 (d, 2H, J = 8.5), 7.65 (d, 2H, J = 8.0), 7.47 (m, 2H), 7.40 (m, 4H).

3-(Pyrazin-2-yl)-*as*-triazino[5,6-*f*]acenaphthylene (dta)

A mixture of cyanodiazine hydrazidine (0.272 g, 2 mmol) and acenaphthenequinone (0.364 g, 2 mmol) was refluxed with stirring in ethanol. A yellow precipitate appeared in a few minutes.

DOI: 10.1039/b208400g

The insoluble material was filtered off after 2 hours, washed with ethanol (2 × 3 cm^3), and dried at 50 °C *in vacuo*. Yield: 0.350 g, 62.0% (Found: C, 71.95; H, 3.24; N, 24.61. Calc. for $C_{17}H_9N_5$: C, 71.82; H, 3.18; N, 24.73%). ^{1}H NMR (CD_2Cl_2): δ 10.03 (s, 1H), 8.94 (s, 1H), 8.81 (s, 1H), 8.75 (d, 1H, J = 7.5), 8.66 (d, 1H, J = 7.0), 8.33 (d, 1H, J = 8.0), 8.26 (d, 1H, J = 8.0), 7.97 (m, 2H). FAB-MS: m/z = 284, $[M + 1]^+$.

3-(Pyrazin-2-yl)-*as*-triazino[5,6-*f*]phenanthrene (dpt)

dpt was synthesized using the same procedure as that described for dta, with 9,10-phenanthraquinone (0.42 g, 2 mmol) in place of acenaphthenequinone. Yield: 0.43 g, 69.0% (Found: C, 73.64; H, 3.64; N, 22.54. Calc. for $C_{19}H_{11}N_5$: C, 73.78; H, 3.56; N, 22.65%). ^{1}H NMR (CD_2Cl_2): δ 10.09 (s, 1H), 9.56 (d, 1H, J = 8.0), 9.47 (d, 1H, J = 8.0), 8.95 (d, J = 5.5, 2H), 8.83 (d, 1H, J = 4.5), 8.65–8.62 (m, 2H), 7.97–7.90 (m, 2H), 7.87–7.80 (m, 2H). FAB-MS: m/z = 310, $[M + 1]^+$.

$[Ru(bpy)_2(ddt)][ClO_4]_2$ 1

A mixture of *cis*-$[Ru(bpy)_2Cl_2]\cdot 2H_2O$ (0.265 g, 0.5 mmol), ddt (0.156 g, 0.5 mmol), ethanol (20 cm^3) and water (10 cm^3) was refluxed under argon for 10 h. After most of the ethanol was removed by rotary evaporation, a brownish red precipitate was obtained by dropwise addition of an excess of $NaClO_4$ solution. The product was purified by column chromatography on alumina using acetonitrile–toluene (1 : 1, v/v) as eluent. Yield: 0.33 g, 72.1% (Found: C, 50.26; H, 3.18; N, 13.49. Calc. for $C_{39}H_{29}Cl_2N_9O_8Ru$: C, 50.70, H, 3.14, N, 13.65%). ^{1}H NMR [$(CD_3)_2SO$]: δ 9.94 (s, 1H), 8.93 (d, 2H, J = 8.5), 8.88 (d, 2H, J = 8.5), 8.85 (m, 1H), 8.78 (d, 2H, J = 8.5), 8.25 (m, 4H), 8.10 (d, 1H, J = 5.0), 8.07 (d, 1H, J = 5.0), 7.80 (d, 1H, J = 5.5), 7.75 (m, 4H), 7.69 (d, 1H, J = 5.0), 7.65 (t, 1H), 7.57 (m, 4H), 7.46 (m, 3H), 7.30 (t, 2H), 7.10 (d, 2H, J = 7.0). MS [ESMS (CH_3CN)]: m/z 824 ($[M - ClO_4]^+$) and 362 ($[M - 2ClO_4]^{2+}$).

$[Ru(bpy)_2(dta)][ClO_4]_2$ 2

This complex was synthesized using the same procedure described for complex **1**, with 0.5 mmol, 0.1415 g dta in place of the ddt. Yield: 0.216 g, 48.2% (Found: C, 48.96; H, 3.02; N, 13.89. Calc. for $C_{37}H_{25}Cl_2N_9O_8Ru$: C, 49.61; H, 2.91; N, 14.08%). ^{1}H NMR [$(CD_3)_2SO$]: δ 9.97 (s, 1H), 8.92 (d, 1H, J = 7.5), 8.88 (d, 1H, J = 8.5), 8.84 (m, 2H), 8.79 (m, 2H), 8.58 (d, 1H, J = 8.0), 8.51 (d, 1H, J = 7.0), 8.28 (q, 2H), 8.21 (t, 1H), 8.15 (m, 4H), 8.02 (d, 1H, J = 7.0), 7.98 (m, 2H), 7.85 (d, 1H, J = 5.0), 7.74 (d, 1H, J = 6.5), 7.76 (t, 1H), 7.62 (t, m), 7.53 (t, 1H), 7.44 (t, 1H). MS [ESMS (CH_3CN)]: m/z 795 ($[M - ClO_4]^+$) and 348 ($[M - 2ClO_4]^{2+}$).

$[Ru(bpy)_2(dpt)][ClO_4]_2$ 3

This complex was synthesized using the same procedure described for complex **1**, with 0.5 mmol, 0.155 g dpt being used instead of ddt. Yieid: 0.25 g, 52.5% (Found: C, 50.18; H, 3.03; N, 13.58. Calc. for $C_{39}H_{27}Cl_2N_9O_8Ru$: C, 50.76; H, 2.93; N, 13.67%). ^{1}H NMR [$(CD_3)_2SO$]: δ 10.28 (s, 1H), 9.57 (d, 1H, J = 7.0), 8.95 (d, 1H, J = 8.5), 8.89 (m, 5H), 8.79 (d, 1H, J = 8.0), 8.38 (t, 1H), 8.29 (t, 1H), 8.21 (t, 1H), 8.16 (m, 5H), 8.07 (m, 4H), 7.81 (d, 1H, J = 6.0), 7.70 (m, 3H), 7.55 (t, 1H), 7.42 (t, 1H). MS [ESMS (CH_3CN)]: m/z 822 ($[M - ClO_4]^+$) and 361 ($[M - 2ClO_4]^{2+}$).

Crystals of dta suitable for X-ray single crystal analysis were obtained by slow evaporation of the ethanol solution at room temperature. Red prismatic crystals of $[Ru(bpy)_2(ddt)][ClO_4]_2$ were grown from the diffusion of diethyl ether vapor into a concentrated acetonitrile solution of the complex.

CAUTION: perchlorate salts of metal complexes with organic ligands are potentially explosive, and only small amounts of the material should be prepared and these should be handled with great care.

Physical measurements

Elemental analyses were carried out with a Perkin-Elmer 240Q elemental analyser. UV–vis spectra were recorded on a Shimadzu MPS-2000 spectrophotometer, emission spectra on a Shimadzu RF-2000 spectrofluorometer and ^{1}H NMR spectra on a Varian INOVA 500 MHz spectrometer. Fast-atom bombardment (FAB) mass spectra were measured on a VG ZAB-HS mass spectrometer with 3-nitrobenzyl alcohol as matrix. Electrospray (ES) mass spectra were recorded on a LCQ system (Finngan MAT, USA) using acetonitrile as mobile phase. The circular dichroism (CD) spectra were measured on a JASCO-J715 spectropolarimeter.

All the experiments involving the interaction of the complexes with DNA were carried out in aerated buffer (5 mmol dm^{-3} Tris-HCl, 50 mmol dm^{-3} NaCl, pH 7.0). Solution of calf thymus DNA (CT-DNA) in the buffer gave a ratio of UV absorbance at 260 and 280 nm of *ca*. 1.9 : 1, indicating that the DNA was sufficiently free of protein. The DNA concentration per nucleotide was determined by absorption spectroscopy using the molar absorption coefficient (6600 dm^3 mol^{-1} cm^{-1}) at 260 nm.

Cyclic voltammetry was performed on an EG&G PAR 273 polarographic analyser equipped with a 270 universal programmer. The supporting electrolyte was 0.1 mol dm^{-3} tetraethylammonium perchlorate in acetonitrile freshly distilled from phosphorus pentaoxide and deaerated by purging with nitrogen. A standard three-electrode system was used comprising platinum microcylinder working electrode, platinum-wire auxiliary electrode and a saturated calomel reference electrode (SCE).

Viscosity experiments were carried on an Ubbelodhe viscometer, immersed in a thermostatic water-bath maintained at a constant temperature of 29 ± 0.1 °C. CT-DNA samples approximately 200 base pairs in length (average) were prepared by sonication in order to minimize complexities arising from DNA flexibility.[11] Data were presented as $(\eta/\eta_0)^{\frac{1}{3}}$ *versus* binding ratio,[12] where η is the viscosity of CT-DNA in the presence of complex, and η_0 is the viscosity of CT-DNA alone. Viscosity values were calculated from the observed flow time of DNA-containing solutions (t) corrected for that of buffer alone (t_0), $\eta = (t - t_0)/t_0$.

Equilibrium dialyses were conducted at room temperature with 5 cm^3 of CT-DNA (1.0 mM) sealed in a dialysis bag and 10 cm^3 of the complexes (50 μM) outside the bag with the solution stirring for 48 h.

For the gel electrophoresis experiments, supercoiled pBR 322 DNA (0.1 μg) was treated with the Ru(II) complexes in 50 mM Tris–acetate, 18 mM NaCl buffer pH 7.2, and the solutions were then irradiated at room temperature with a UV lamp (440 nm, 10 W). The samples were analysed by electrophoresis for 3 h at 25 V on a 1% agarose gel in Tris–acetate buffer. The gel was stained with ethidium bromide and photographed under UV light.

X-Ray crystallography

Experimental details of the X-ray analyses are provided in Table 1. Diffraction data were collected on a Bruker Smart 1000 CCD diffractometer equipped with graphite monochromated Mo-Kα radiation (λ = 0.71073 Å) at room temperature. Absorption corrections for complex **1** and dta were applied by SADABS.[13] The structures were solved by direct methods and refined using full-matrix least-squares/difference Fourier techniques using SHELXTL.[14] All non-hydrogen atoms were refined with anisotropic displacement parameters. After that, all hydrogen atoms of the ligands were placed at idealized positions and refined as riding atoms with the relative isotropic parameters of the heavy atoms to which they are attached.

Crystal parameters and details of the data collection and refinement are given in Table 1. Selected bond lengths (Å) and bond angles (°) are given in Table 2.

Table 1 Crystal and structure refinement for ligand dta and complex **1**

	dta	**1**
Chemical formula	$C_{17}H_9N_5$	$C_{39}H_{29}Cl_2N_9O_8Ru$
Formula weight	283.29	923.68
Crystal system	Monoclinic	Monoclinic
Space group	*Cc*	$P2_1/c$
a/Å	11.133(10)	14.505(3)
b/Å	26.01(2)	11.556(2)
c/Å	13.574(12)	23.864(5)
β/°	106.140(16)	98.85(3)
V/Å^3	3775(6)	3952.5(13)
Z	2	4
F(000)	1752	1872
μ/mm^{-1}	0.095	0.58
Measured/independent reflections and *R*(int)	11008, 4092, 0.0384	23100, 8682, 0.0295
*R*1 [$I > 2\sigma(I)$]	0.0467	0.0440
*w R*2 [$I > 2\sigma(I)$]	0.1227	0.1040

CCDC reference numbers 192534 and 192535.

See http://www.rsc.org/suppdata/dt/b2/b208400g/ for crystallographic data in CIF or other electronic format.

Results and discussion

Crystal structures

[Ru(bpy)$_2$(ddt)][ClO$_4$]$_2$ 1. As shown in Fig. 1, the Ru(II) ion is chelated by two bpy ligands in a *cis* fashion and a ddt ligand. The overall structure of the complex cation can be described as a distorted octahedron, with an average bite angle of 78.6° for the three bidentate ligands. The mean Ru–N (bpy) distance is 2.072 Å, similar to that found in $[Ru(bpy)_3]^{2+}$ (2.056 Å).[15] However, the two Ru–N distances of the ddt ligand are significantly different. The Ru–N(1) distance (2.050 Å) is similar to that of Ru–N (bpy), while the Ru–N(3) distance is 2.026 Å. The inequivalence of the two Ru–N bonds indicates that the 1,2,4-triazine group has a stronger coordination ability than the pyrazine. In addition, the two phenyl rings in ddt are rotated away from the 1,2,4-triazine ring, forming dihedral angles of 45.9° and 42.5° with the 1,2,4-triazine ring plane.

The crystal structure of dta is depicted in Fig. 2. All C–N and C–C bond distances are in the normal range. What we are most interested in is the planarity of the molecule. The naphthyl ring is nearly coplanar with the 1,2,4-triazine ring and can construct a larger π framework than the ddt ligand.

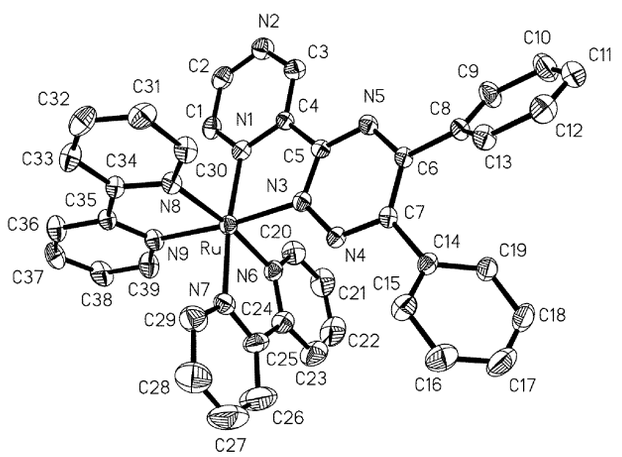

Fig. 1 An ORTEP[26] drawing of complex **1** and the atom numbering.

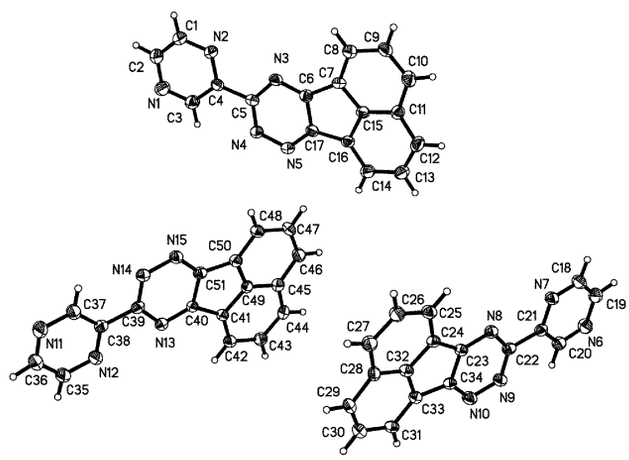

Fig. 2 An ORTEP drawing of dta and the atom numbering.

Electrochemistry

The electrochemical behaviors of complexes **1**, **2** and **3** were investigated in acetonitrile. The results are listed in Table 3. Cyclic voltammetry of complexes **1**, **2** and **3** shows one oxidation and three reduction waves in the sweep range from −1.80 to 1.80 V (*vs.* SCE). The electrochemical behavior of the complexes has been rationalized in terms of metal-based oxidation and a series of reductions which are ligand-based occurring in a stepwise manner to each π*-system. The oxidation potentials of complexes **1**, **2** and **3** become less positive in the order of coordinated ligand dpt > dta > ddt. This observation suggests that the better the π* acceptor characteristics of the ligand (ddt, dta or dpt) the more stable the ruthenium-based HOMO becomes, rendering the oxidation of the metal cation more

Table 2 Select bond lengths (Å) and angles (°) for dta and complex **1**

dta							
N(1)–C(2)	1.330(9)	N(1)–C(3)	1.324(8)	N(2)–C(1)	1.329(7)	N(5)–C(17)	1.312(7)
N(2)–C(4)	1.344(7)	N(3)–C(6)	1.306(7)	N(3)–C(5)	1.353(8)	N(4)–N(5)	1.360(6)
N(4)–C(5)	1.321(8)						
N(3)–C(6)–C(7)	129.4(5)	N(2)–C(4))–C(5)	117.1(5)	N(4)–C(5)–C(4)	115.1(5)	N(5)–C(17)–C(6)	121.4(5)
C(8)–C(7)–C(6)	135.7(6)	C(15)–C(7)–C(6)	105.7(5)	C(11)–C(15)–C(7)	124.2(5)	C(17)–C(6)–C(7)	108.3(4)
C(15)–C(16)–C(17)	105.4(5)	C(6)–C(17)–C(16)	108.2(5)	N(5)–C(17)–C(16)	130.3(5)	C(10)–C(9)–C(8)	122.8(7)
1							
Ru–N(1)	2.050(3)	Ru–N(3)	2.026(3)	Ru–N(6)	2.070(3)	Ru–N(9)	2.076(3)
Ru–N(7)	2.071(3)	Ru–N(8)	2.074(3)				
C(1)–N(1)–Ru	128.6(3)	C(4)–N(1)–Ru	115.3(3)	N(4)–N(3)–Ru	122.9(2)	N(3)–Ru–N(8)	97.58(11)
C(5)–N(3)–Ru	117.1(2)	C(20)–N(6)–Ru	125.8(3)	C(24)–N(6)–Ru	115.5(3)	N(1)–Ru–N(8)	86.15(11)
N(3)–Ru–N(3)	78.47(11)	N(3)–Ru–N(9)	174.34(11)	N(1)–Ru–N(9)	96.97(11)	N(9)–Ru–N(9)	78.65(12)
N(3)–Ru–N(6)	88.16(11)	N(1)–Ru–N(6)	99.10(12)	N(6)–Ru–N(9)	95.92(12)	N(6)–Ru–N(8)	172.93(12)
N(3)–Ru–N(7)	95.01(11)	N(1)–Ru–N(7)	173.21(11)	N(7)–Ru–N(9)	89.66(12)	N(7)–Ru–N(8)	96.66(12)
N(6)–Ru–N(7)	78.66(13)						

Table 3 Electrochemical potential for ruthenium(II) complexes

Complex	Oxidation[a] $E_{1/2}$/V	Reduction[a] $E_{1/2}$/V		
		I	II	II
1	1.32	−0.91	−1.39	−1.65
2	1.36	−0.96	−1.41	−1.68
3	1.39	−1.01	−1.44	−1.69
$[Ru(bpy)_3]^{2+}$	1.27	−1.31	−1.50	−1.77

[a] Redox potentials are quoted *vs.* SCE in 0.1 M TBAH–CH_3CN. Scan rate = 200 mV s^{-1}.

difficult. The first reduction, which is usually controlled by the ligand having the most stable lowest unoccupied molecular orbital (LUMO)[16] is proposed to be the asymmetric ligand-centered (ddt, dta or dpt) reduction. The latter two successive reductions are characteristic of the co-ligand (bpy).[17]

Absorption spectra

The absorption spectra of complexes **1**, **2** and **3** in the absence and presence of CT-DNA at various complex concentrations are given in Fig. 3. The spectra of the three complexes consist of three or four well-resolved bands in the range 200 to 600 nm. All of them display a strong MLCT band at 400–600 nm attributed to the overlap of Ru(II) ⟶ bpy (π*) and Ru(II) ⟶ ddt, dta or dpt (π*). At higher energy (320–390 nm), the spectra display a sharp band, corresponding to (ddt, dta or dpt)–π* and π–π* transitions . Below 320 nm, the strong bands can be attributed to (bpy) π–π*.[18]

With increasing DNA concentration, the hypochromism increases and is accompanied by a red shift in the MLCT band of the complexes. These results are similar to those reported earlier for various metallointercalators[19] and suggest that the three complexes bind strongly to DNA in an intercalative mode. The percentages of hypochromism in the visible MLCT band for the Ru(II) complexes in the presence of DNA at saturation are listed in Table 4. In order to compare quantitatively the binding strength of the three complexes, their intrinsic binding constants with CT-DNA were obtained by monitoring the changes in absorbance at 467, 500 and 474 nm for complexes **1**, **2** and **3** respectively, with increasing concentration of DNA. The following equation was applied:[20]

$$[DNA]/(\varepsilon_a - \varepsilon_b) = [DNA]/(\varepsilon_b - \varepsilon_f) + 1/K_b(\varepsilon_b - \varepsilon_f)$$

where [DNA] is the concentration of DNA in base pairs, the apparent absorption coefficients ε_a, ε_f, and ε_b correspond to A_{obsd}/[Ru], the extinction coefficient for the free ruthenium complex, and the extinction coefficient for the ruthenium complex in the fully bound form, respectively. Plots of [DNA]/($\varepsilon_a - \varepsilon_b$) *versus* [DNA] gave a slope of $1/(\varepsilon_a - \varepsilon_b)$, and the intercept equals $1/K_b(\varepsilon_b - \varepsilon_f)$; K_b is the ratio of the slope to the intercept. Intrinsic binding constants K_b of $(2.1 \pm 0.3) \times 10^4$ M^{-1}, $(3.7 \pm 0.4) \times 10^4$ and $(6.3 \pm 0.4) \times 10^4$ M^{-1} were obtained for complexes, **1**, **2** and **3**, respectively. The binding constants show the following ordering: **3** > **2** > **1**. In general, a planar

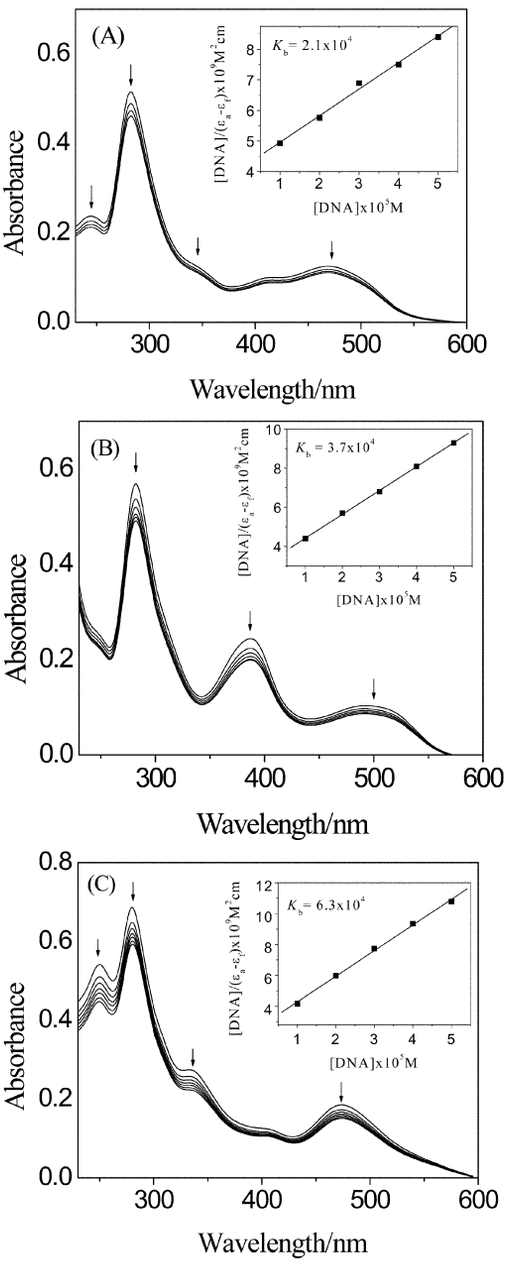

Fig. 3 Absorption spectra of complexes **1** (A), **2** (B) and **3** (C) in 50 mM Tris-HCl and 50 mM NaCl buffer (pH = 7.2) in the presence of increasing amounts of DNA (Ru = 10 μM, [DNA] = 0–100 μM).

extension of the intercalative ligand would increase the strength of the interaction of the complexes with DNA.[21] This significant difference in DNA binding affinity of complexes **1**–**3** can be understood as a result of the fact that the dta and dpt ligands display a more planar conjugate system than that of the ddt ligand.

Unfortunately, complexes **1**–**3** do not show any photoluminescence at room temperature in any organic solvent examined,

Table 4 Electronic absorption data upon addition of CT-DNA

Complex	λ_{max}/nm				Binding constant
	Free	Bound	Δλ	Hypochromism, H^a(%)	K_b/M^{-1}
1	467	469	2	9.5	$(2.1 \pm 0.3) \times 10^4$
2	500	504	4	13.1	$(3.7 \pm 0.4) \times 10^4$
3	474	479	5	18.1	$(6.3 \pm 0.4) \times 10^4$

[a] $H\% = 100(A_{free} - A_{bound})/A_{free}$.

in the absence or presence of DNA. The detailed mechanism is unclear.

Viscosity measurements

Optical photophysical probes generally provide necessary, but not sufficient, evidence to support the binding mode of Ru(II) complexes with DNA. To further clarify the nature of the interaction between the complexes and DNA, viscosity measurements were carried out and the results presented in Fig. 4.

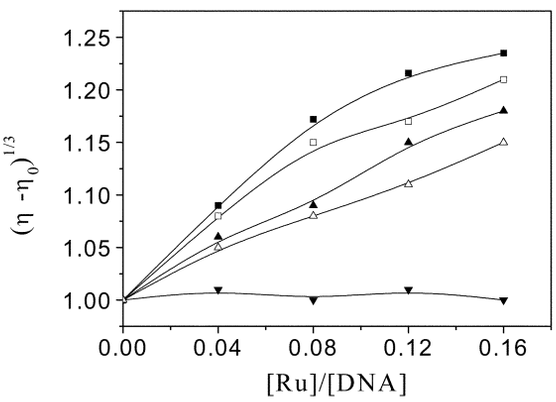

Fig. 4 Effect of increasing amounts of $[Ru(bpy)_2(dppz)]^{2+}$ (■), **3** (□), **2** (▲), **1** (△) and $[Ru(bpy)_3]^{2+}$ (▼) on the relative viscosity of calf thymus DNA at 29 ± 0.1 °C.

Intercalation is expected to lengthen the DNA helix as the base pairs are pushed apart to accommodate the bound ligand, leading to an increase in the DNA viscosity. In contrast, a partial, non-classical intercalation of ligand could bend (or kink) the DNA helix, reduce its effective length and, concomitantly, its viscosity.[22,23] The viscosity of DNA bound to complexes **1**, **2**, and **3** is increased with the increment of the complex concentration, which is similar to the behavior of the known DNA intercalator $[Ru(bpy)_2(dppz)]^{2+}$ (dppz = dipyridophenazine).[8c] On the other hand, for $[Ru(bpy)_3]^{2+}$, which has been well known to bind with DNA through the eletrostatic mode, there is no effect on the relative viscosity of the DNA solution. The experimental results suggest that all three complexes intercalate the base pairs of DNA. The viscosity of DNA bound with complex **3** increases dramatically but is still smaller than that reported for $[Ru(bpy)_2(dppz)]^{2+}$. A smaller increase is observed for complex **1** compared with those of complex **2** and **3**, and complex **3** is the most efficient intercalator.

Enantioselectivity of binding to DNA

Equilibrium dialysis experiments may offer the opportunity to examine the enantioselectivity of complex binding to DNA. According to the insertion model proposed by Barton,[1e] the Δ enantiomer of the complex, a right-handed propeller-like structure, will display a greater affinity than the Λ enantiomer with the right-handed CT-DNA helix, due to appropriate steric matching.

The CD spectra in the UV region of complexes **2** and **3** after their racemic solutions were dialysed against CT-DNA are shown in Fig. 5. The dialysate shows two CD signals with a positive peak at 269 and 270 nm, and a negative peak at 287 and 290 nm, for complexes **2** and **3**, respectively. However the CD spectra for the dialysate of complex **1** show no discernible signals. Therefore, the CD results indicate that complexes **2** and **3** interact enantioselectively with calf thymus DNA, but not complex **1**.

DNA photocleavage

There has been considerable interest in DNA endonucleolytic cleavage reactions that are activated by metal ions.[24] The

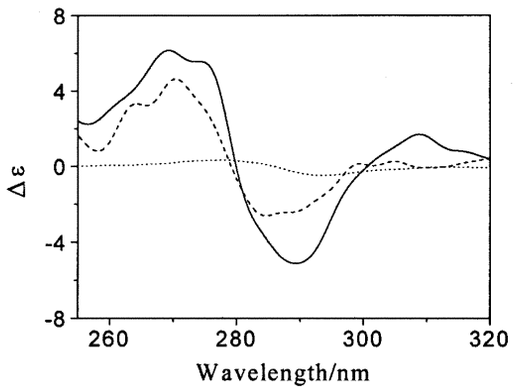

Fig. 5 The CD spectra of the dialysates of **3** (—), **2** (---) and **1** (· · ·) after 48 h of dialysis against CT-DNA ([Ru] = 50μM, [DNA] = 1.0 mM).

cleavage reaction on plasmid DNA can be monitored by agarose gel electrophoresis. When circular plasmid DNA is subject to electrophoresis, relatively fast migration will be observed for the intact supercoil form (Form I). If scission occurs on one strand (nicking), the supercoil will relax to generate a slower-moving open circular form (Form II). If both strands are cleaved, a linear form (Form III) that migrates between Form I and Form II will be generated.[25] Fig. 6 shows gel electrophoresis separation of pBR 322 DNA after incubation with the three Ru(II) complexes and irradiation at 365 nm. Lane 0 is the control group with DNA alone. With increasing concentration of complexes **2** and **3** (lanes 4–9), Form I of pBR 322 DNA diminishes gradually, whereas the amount of Form II increases and Form III is also produced in (lane 9). While **2** induced the single-strand scissions in supercoiled DNA, **3** induced the double-strand scissions. On the other hand, in the presence of **1** (lanes 1–3), no distinct cleavage of pBR 322 DNA is observed. Under comparable experimental conditions, DNA-nicking efficiencies of these complexes follow the trend **3** > **2** > **1**. This result may be related to the absorption intensity at 365 nm and the affinity for DNA. Further study is necessary to clarify the reaction mechanism.

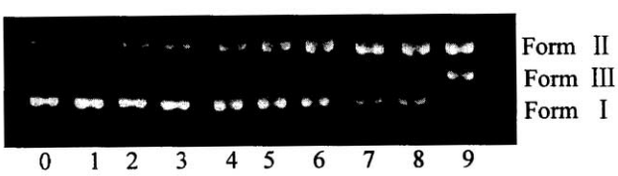

Fig. 6 Photograph showing the effect of ruthenium(II) complexes and light on supercoiled pBR 322 DNA after incubation for 1 h at 37 °C. DNA alone (lane 0), the concentration of **1** was 20, 40, 60 μM (lanes 1–3); the concentration of **2** was 20, 40, 60 μM (lanes 4–6); the concentration of **3** was 20, 40, 60 μM (lanes 7–9).

Conclusion

In summary, three new Ru(II) complexes $[Ru(bpy)_2(ddt)][ClO_4]_2$, (**1**), $[Ru(bpy)_2(dta)][ClO_4]_2$ **2** and $[Ru(bpy)_2(dpt)][ClO_4]_2$ **3** have been synthesized and characterized. The experimental results of spectra titration and viscosity measurements suggest that the three complexes bind to DNA in the classical intercalated binding mode. The DNA binding affinity follows the order **3** > **2** > **1**. When irradiated at 365 nm, both complexes **2** and **3** are efficient photocleavers of the plasmid. These complexes may be useful as tools for probing DNA structure.

Acknowledgements

We are grateful to the National Natural Science Foundation of China, the Natural Science Foundation of Guangdong

Province, the State Key Laboratory of Coordination Chemistry at Nanjing University and the Research Fund of Royal Society of Chemistry UK for their financial support.

References

1 (*a*) L. De Cola and P. Belser, *Coord. Chem. Rev.*, 1998, **177**, 301; (*b*) V. Balzani, A. Juris, M. Venturi, S. Campagna and S. Serroni, *Chem. Rev.*, 1996, **96**, 756; (*c*) K. E. Duncan, D. T. Odom and J. K. Barton, *Chem. Rev.*, 1999, **99**, 2777; (*d*) F. R. Keene, *Coord. Chem. Rev.*, 1997, **166**, 121; (*e*) J. K. Barton, *Science*, 1986, **233**, 727.

2 R. Hage, R. Prins, J. G. Hassnoot and J. Reedijk, *J. Chem. Soc., Dalton Trans.*, 1987, 1389; P. J. Steel, F. Lahousse, D. Lerner and C. Marzin, *Inorg. Chem.*, 1983, **22**, 1488; G. Orellana, C. Ibarra and J. Santoro, *Inorg. Chem.*, 1988, **27**, 1025; C. Hiort, P. Lincoln and B. Norden, *J. Am. Chem. Soc.*, 1993, **115**, 3448; I. Haq, P. Lincoln, D. Suh, B. Norden, B. Z. Chowdhry and J. B. Chair, *J. Am. Chem. Soc.*, 1995, **117**, 4788; P. Lincoln, A. Broo and B. Norden, *J. Am. Chem. Soc.*, 1996, **118**, 2644.

3 X. H. Zou, B. H. Ye, H. Li, J. G. Liu, Y. Xiong and L. N. Ji, *J. Chem. Soc., Dalton Trans.*, 1999, 1423.

4 R. J. Morgan, S. Chatterjee, A. D. Baker and T. C. Strekas, *Inorg. Chem.*, 1991, **30**, 2687.

5 A. M. Pyle, J. P. Rehmann, R. Meshoyrer, C. V. Kumar, N. J. Turro and J. K. Barton, *J. Am. Chem. Soc.*, 1989, **111**, 3051; R. H. Harsh and J. K. Barton, *J. Am. Chem. Soc.*, 1992, **114**, 5919.

6 D. Ossipov, P. I. Pradeepkumar, M. Holmer and J. Chattopadhyaya, *J. Am. Chem. Soc.*, 2001, **123**, 3551; P. K. Bhattacharya and J. K. Barton, *J. Am. Chem. Soc.*, 2001, **123**, 8649.

7 Y. Xiong and L. N. Ji, *Coord. Chem. Rev.*, 1999, **185–186**, 711.

8 (*a*) J. G. Liu, B. H. Ye, Q. L. Zhang, X. H. Zou, Q. X. Zhen, Q. X. Tian and L. N. Ji, *J. Biol. Inorg. Chem.*, 2000, **5**, 119; (*b*) X. H. Zou, B. H. Ye, H. Li, Q. L. Zhang, H. Chao, J. G. Liu, L. N. Ji and X. Y. Li, *J. Biol. Inorg. Chem*, 2001, **6**, 143; (*c*) J. G. Liu, Q. L. Zhang, X. F. Shi and L. N. Ji, *Inorg. Chem*, 2001, **40**, 5045; (*d*) X. H. Zou, H. Li, G. Yang, H. Deng, J. Liu, R. H. Li, Q. L. Zhang, Y. Xiong and L. N. Ji, *Inorg. Chem.*, 2001, **40**, 7091.

9 B. P. Sullivan, D. J. Salmon and T. J. Meyer, *Inorg. Chem.*, 1978, **17**, 3334.

10 F. H. Case, *J. Heterocycl. Chem.*, 1968, **5**, 223.

11 J. B. Chaires, N. Dattagupta and D. M. Crothers, *Biochemistry*, 1982, **21**, 3933.

12 G. Cohen and H. Eisenberg, *Biopolymers*, 1969, **8**, 45.

13 R. Blessing, *Acta Crystallogr., Sect. A*, 1995, **51**, 33–38.

14 (*a*) Bruker AXS, SHELXTL, Version 5.1, Bruker AXS, Madison, WI, 1991; (*b*) G. M. Sheldrick, SHELX97, Program for X-ray Crystal Structure Solution and Refinement, Göttingen University, Germany, 1997.

15 D. P. Rillema, D. S. Jones and H. A. Levy, *J. Chem. Soc., Chem. Commun*, 1979, 849; D. P. Rillema, D. S. Jones, C. Woods and H. A. Levy, *Inorg. Chem.*, 1992, **31**, 2935.

16 D. P. Rillema, G. Allen, T. J. Meyer and D. C. Conrad, *Inorg. Chem.*, 1983, **22**, 1617.

17 B. K. Ghosh and A. Chakravorty, *Coord. Chem. Rev.*, 1989, **95**, 239.

18 J. Bolger, A. Gourden, E. Ishow and J. P. Launay, *Inorg. Chem.*, 1996, **35**, 2937.

19 E. C. Long and J. K. Barton, *Acc. Chem. Res.*, 1990, **23**, 271.

20 A. Wolfe, G. H. Shimer and T. Meehan, *Biochemistry*, 1987, **26**, 6392.

21 A. M. Pyle, J. K. Barton, in S. J. Lippard (Editor), *Progress in Inorganic Chemistry: Bioinorganic Chemistry*, Wiley, New York, 1990, vol. 38, p. 413.

22 S. Satyanarayana, J. C. Dabrowiak and J. B. Chaires, *Biochemistry*, 1992, **31**, 9319.

23 S. Satyanarayana, J. C. Dabrowiak and J. B. Chaires, *Biochemistry*, 1993, **32**, 2573.

24 D. S. Sigman, D. R. Graham, L. E. Marshall and K. A. Reich, *J. Am. Chem. Soc.*, 1980, **102**, 5419.

25 J. K. Barton and A. L. Raphael, *J. Am. Chem. Soc.*, 1984, **106**, 2466.

26 C. K. Johnson, ORTEP-II: A FORTRAN Thermal Ellipsoid Plot Program for Crystal Structure Illustrations, Report ORNL-5138, Oak Ridge National Laboratory, Oak Ridge, TN, USA, 1976.